Optimization of Extracellular Vesicle Release for Targeted Drug Delivery

Martin Damrath, Mladen Veletić, *Member, IEEE*, Hamid Khoshfekr Rudsari, and Ilangko Balasingham, *Senior Member, IEEE*

***Abstract*— Targeted drug delivery is a promising approach for many serious diseases, such as glioblastoma multiforme, one of the most common and devastating brain tumor. In this context, this work addresses the optimization of the controlled release of drugs which are carried by extracellular vesicles. Towards this goal, we derive and numerically verify an analytical solution for the end-to-end system model. We then apply the analytical solution either to reduce the disease treatment time or to reduce the amount of required drugs. The latter is formulated as a bilevel optimization problem, whose quasiconvex/quasiconcave property is proved here. For solving the optimization problem, we propose and utilize a combination of bisection method and golden-section search. The numerical results demonstrate that the optimization can significantly reduce the treatment time and/or the required drugs carried by extracellular vesicles for a therapy compared to the steady state solution.**

***Index Terms*— Extracellular vesicle, glioblastoma, joint optimization, molecular communication, targeted drug delivery.**

I. Introduction

The research area of molecular communications deals with the biologically-inspired way of transmitting information by means of molecules. One of the cutting-edge applications of this concept is in targeted drug delivery (TDD) [1], where molecules can be used to regulate drug release and/or act as the drug themselves. As a result, the drug release can take place locally at the site of the diseased cells and in proper quantity over an appropriate time. This enables a reduction of adverse effects, a personalized treatment improving the therapeutic effect, and thus opens a new era of drug treatment. Molecular communication can be used in this application to control and coordinate the release of the drug or for tracking and navigation to the local target. Furthermore, the release of the drug, its transport, uptake as well as achieved effects at the target site can be abstracted and treated as a molecular communication system, based on the transmitter, channel, and receiver.

This work assumes but is not limited to a TDD scenario for a brain tumor, where cell-derived extracellular vesicles (EVs) are used as vehicles to deliver therapeutic cargo to cancer cells [2], [3]. EVs are lipid bilayer-delimited particles on the order of $20\,\mathrm{nm}$ to $10\,\mu\mathrm{m}$. They are biologically tolerable, can be target-specific, and serve as vehicles for therapeutic molecules such as micro ribonucleic acids (RNAs), which they protect from various environmental factors (e.g., enzymes). At the cancer cell, the EVs act as a Trojan horse, which is internalized and degraded, wherein their cargo can interfere with the underlying disease pathway. Here, we address the optimization of EV release from originating cells with respect to a therapeutic effect, which is important to provide the discussed personalized treatment and to control/minimize adverse effects. In addition, the release can be adapted to the urgency of the treatment or the synthesis of EVs.

In the literature, there are several papers dealing with the optimization of TDD systems. The considered optimization criteria can be roughly divided into two categories. The first category describes the problem from a communication theoretic point of view and tries to optimize typical quantities such as intersymbol interference [4], bit error rate [4], [5], or throughput [6]. While these quantities are interesting for Shannon information transfer, they provide only limited information about the therapeutic effect of the drug at the target. The second category takes a more direct approach and optimizes the drug concentration level in the target cell to guarantee a therapeutic effect [7]–[9]. The corresponding works mainly consider steady state solutions. Although they do not optimize the initial concentration rise, which occurs at the start of a therapy and is necessary to obtain a target concentration level, they bear a lot of potential in suggesting how to either save resources in form of released drugs or to enable fast treatment. Hence, we address the optimization of the initial EV concentration rise in target cells, here cancer cells, using a specific brain tumor (glioblastoma multiforme) as a case study. The novel contributions can be summarized

Manuscript received October 14, 2022. This work was supported by the EU (EU-H2020-FETOpen GLADIATOR—Next-generation Theranostics of Brain Pathologies with Autonomous Externally Controllable Nanonetworks: A Trans-disciplinary Approach with Bio-nanodevice Interfaces) under Grant #828837 and by the Research Council of Norway (RCN: CIRCLE Communication Theoretical Foundation of Wireless Nanonetworks) under Grant 287112.

M. Damrath is with the Department of Electronic Systems, Norwegian University of Science and Technology, 7491 Trondheim, Norway (e-mail: martin.damrath@ntnu.no).

M. Veletić and I. Balasingham are with the Department of Electronic Systems, Norwegian University of Science and Technology, 7491 Trondheim, Norway, and also with the Intervention Centre, Oslo University Hospital, 0027 Oslo, Norway (e-mail: mladen.veletic@ntnu.no; ilangko.balasingham@ntnu.no).

H. K. Rudsari is with the Faculty of Medicine, Institute of Clinical Medicine, University of Oslo, 0316 Oslo, Norway, and also with the Intervention Centre, Oslo University Hospital, 0027 Oslo, Norway (e-mail: h.k.rudsari@studmed.uio.no).

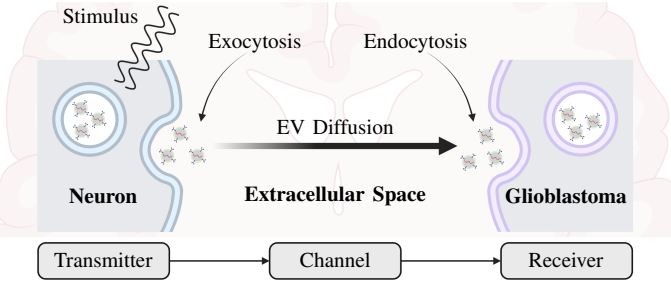

Fig. 1. The EV-mediated brain drug delivery molecular communication system model. The illustration was created using BioRender.com.

as follows:

- A time-domain analytical solution for the end-to-end model (detailed in Sec. II) is derived incorporating the existing endocytosis (the EV uptake) model [2]. It is demonstrated that the exact exocytosis (the EV release) model [3] can be replaced by its averaged dynamics in the end-to-end model.
- The rise in drug concentration within the target cell is optimized with respect to a target concentration, in contrast to the existing works [4]–[9]. The cases of fastest possible treatment and drug conserving treatment are considered.
- The optimization is formulated as a bilevel optimization problem. It is further proved that the problem is at least quasiconvex/quasiconcave and an algorithm combining bisection method and golden-section search is proposed to solve the problem.

The remainder of the paper is organized as follows. In Sec. II, the EV-mediated brain drug delivery molecular communication system model is described and the analytical solution for the end-to-end model in the time domain is derived. This serves as the basis for the formulation of the drug release optimization as a bilevel optimization problem and its solution algorithm, which are given in Sec. III. In Sec. IV, numerical results are used to verify the end-to-end model and to demonstrate and discuss the potential of optimizing the initial concentration rise. Finally, the paper is concluded in Sec. V.

II. The EV-mediated Brain Drug Delivery Molecular Communication System Model

Fig. 1 gives an overview of the system model under investigation using glioblastoma multiforme as an example application. For the sake of simplicity, we consider a point-to-point transmission in this study. However, the concept can be extended to multipoint transmission in future works. A neuron acts as the transmitter of therapeutic EVs within the considered TDD system. Neurons, like many other cells, naturally synthesize EVs and release them into their environment [10]. The cargo of EVs contain, among others, genetic material such as messenger RNA, micro RNA, short interfering RNA, and genomic deoxyribonucleic acid [11]. These genetic materials are known to play an important role in cell-to-cell signaling and to achieve a potential therapeutic effect by interfering with disease pathways inside cancer cells [12]. Based on these insights, one treatment approach is the reprogramming of somatic cells to create induced neural stem cells (i-NSCs) that are engineered to deliver anticancer molecules present in the synthesized and released EVs [13]. These iNSCs will typically differentiate into neurons and astrocytes [14]. It should be mentioned that the practical implementation of such modifications is outside the scope of this work, but the interested reader is referred to [15] and references therein. The assumption relevant for this study is that wavelength-dependent promoters are incorporated into the therapeutic EV-releasing neuron [3]. Consequently, the neuron can be stimulated by an external electromagnetic signal, which further regulates neural spiking and, subsequently, the EV release accomplished via the mechanism called *exocytosis*. The released EVs diffuse through the extracellular matrix (ECM) of the brain to the targeted glioblastoma cell and enter the cell via the mechanism called *endocytosis*. Inside the cell, the therapeutic cargo, for example micro RNA, is released and interferes with the disease pathway.

In the following, we describe the transmitter, channel, and receiver with respect to their assumptions. In addition to their transfer functions in the Laplace domain, we present their time domain representation.

A. Transmitter

Throughout this paper, a neuron is assumed as the transmitter. However, the results can be extended to other neural cells, e.g., astrocytes, with little effort as shown in [3]. Due to the promoters, the external stimulus will lead to depolarization of the neuron cell membrane and, if intense enough, to the generation of an action potential. The latter follows an all-or-nothing principle and the intensity of the stimulus does not affect the amplitude but only the frequency of the generated action potentials. The maximum frequency is thereby limited by the minimal refractory period of a neuron to $500\,\mathrm{Hz}$ [16]. Depolarization also leads to an increase in exocytosis of EVs [17], and thus can be exploited for regulation of EV release. For simplicity, but without loss of generality, we assume that the neuron will not spontaneously generate action potentials.

For this study, we consider the action potential-based changed release rate of EVs presented in [3][1] as approximately described by a decaying exponential function. Since internalization as part of endocytosis is the rate-limiting process [18], the exact shape of the EV release does not have a significant impact on the end-to-end behavior and an approximation is not critical, as we discuss in more detail in Sec. IV-B. Furthermore, the exponential function has a simple Laplace transform and thus can be easily tracked mathematically. Fig. 2 shows an example of the EV release rate in response to a stimulus that generates K action potentials with a frequency of $1/T$ as

$$x(t) = c_{\min} + (c_{\max} - c_{\min}) \times \sum_{k=0}^{K-1} \exp\left(-\gamma(t - kT)\right) \Theta(t - kT), \quad (1)$$

where the parameter $\gamma > 0$ determines the strength of the exponential decay, $c_{\max}$ is the maximum EV release rate, and

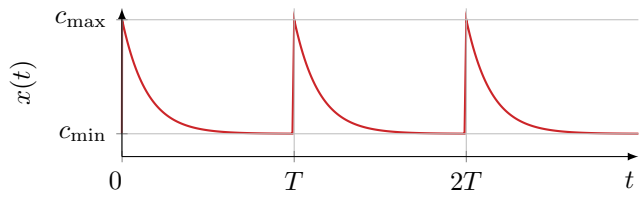

Fig. 2. EVs release rate in response to a stimulus that generates action potentials with a frequency of $\mathbf{1}/\boldsymbol{T}$.

$\Theta(t)$ denotes the Heaviside step function. Even when neurons are not excited, they release $c_{\min}$ of EVs, which corresponds to the so-called baseline EV release rate. The corresponding representation in the Laplace domain is

$$X(s) = \frac{c_{\min}}{s} + (c_{\max} - c_{\min}) \sum_{k=0}^{K-1} \frac{\exp(-kTs)}{s+\gamma}. \quad (2)$$

In the limit, when K increases ($K \to \infty$), the averaged EV release rate is

$$\begin{aligned} \bar{c} &= c_{\min} + \frac{c_{\max} - c_{\min}}{T} \int_0^{\infty} \exp(-\gamma t)\, \mathrm{d}t \\ &= c_{\min} + \frac{c_{\max} - c_{\min}}{\gamma T}. \end{aligned} \quad (3)$$

B. Channel

EVs released by exocytosis propagate by diffusion in the ECM of the brain. The propagation of a released EV, under the assumption of isotropic propagation and no degradation, can be described by the channel impulse response [2][1]

$$h_{\mathrm{c}}(t) = \frac{\lambda^3}{\alpha(4\pi D t)^{3/2}} \exp\left(-\frac{\lambda^2 d^2}{4Dt}\right) \Theta(t), \quad (4)$$

where D is the free diffusion coefficient, and d is the distance to the initial release point at $t = 0$. The parameters λ and α describe the effect of tortuosity and volume fraction, respectively. Tortuosity indicates the ratio of propagation in an obstacle-free medium to effective propagation in a complex medium such as the ECM of the brain. Thereby $\lambda = 1$ is equivalent to an obstacle-free medium and $\lambda = \infty$ is equivalent to an impenetrable medium. Volume fraction describes the ratio of the volume of a medium, such as the ECM of the brain, in which EVs can propagate, to the total volume of tissue. While $\alpha = 0$ is equivalent to an absence of the ECM of the brain, $\alpha = 1$ represents brain tissue consisting exclusively of the ECM of the brain. The Laplace transform of (4) gives the channel transfer function

$$H_{\mathrm{c}}(s) = \frac{\lambda^2}{4\pi d\alpha D} \exp\left(-\lambda d\sqrt{\frac{s}{D}}\right). \quad (5)$$

[1]For more details on the established models and their underlying assumptions, we kindly refer the interested reader to our previous work.

C. Receiver

When the EVs reach the glioblastoma cell, they may be internalized by the cell and their cargo released. Internalization can occur by several different processes. In this work, we focus on the internalization mechanism referred to as the clathrin-dependent receptor-mediated endocytosis [2]. Assuming that the concentration of clathrin-coated pits N is constant and taking into account the first-order kernel of the Volterra Series, the receiver impulse response and receiver transfer function can be modeled respectively by [2][1]

$$h_{\mathrm{r}}(t) = k_{\mathrm{i}} a p_{\mathrm{m}} N \frac{\exp(-k_{\mathrm{i}} t) - \exp(-k_{\mathrm{d}} t)}{k_{\mathrm{d}} - k_{\mathrm{i}}} \Theta(t), \quad (6)$$

$$H_{\mathrm{r}}(s) = \frac{k_{\mathrm{i}} a p_{\mathrm{m}} N}{(k_{\mathrm{d}} + s)(k_{\mathrm{i}} + s)}, \quad (7)$$

where N denotes the concentration of clathrin-coated pits, p_{m} the maximum number of receptors per pit, a the rate at which EVs bind to the receptor, k_{i} the internalization rate, and k_{d} the degradation rate of EVs.

D. End-to-End Model

We aim here to optimize the release of the drug-carrying EVs with respect to the therapeutic effect in the cancer cell. To achieve this goal, having an end-to-end model that describes the input-output behavior of the system is essential. The input of the system represents the EV release rate $x(t)$ at the transmitter. The output is the resulting internalized EV concentration $y(t)$ at the receiver. Assuming that the system is (at least approximately) linear and time-invariant, $y(t)$ and its Laplace transform $Y(s)$ can be calculated as

$$y(t) = (x * h_{\mathrm{c}} * h_{\mathrm{r}})(t), \quad (8)$$

$$Y(s) = X(s) H_{\mathrm{c}}(s) H_{\mathrm{r}}(s). \quad (9)$$

The complex evaluation of the convolutions in the time domain can be avoided by a simple multiplication in the Laplace domain and a subsequent inverse transformation. The internalization of EVs in endocytosis is the rate-limiting process and is comparatively much slower than the release of EVs at the transmitter [18]. Consequently, as we additionally investigate in Sec. IV-B, $X(s)$ can be well approximated by its averaged EV release rate in (3) to

$$X(s) \approx \frac{\bar{c}}{s} = \bar{X}(s) \quad (10)$$

and thus results in

$$\begin{aligned} \bar{Y}(s) &= \bar{X}(s) H_{\mathrm{c}}(s) H_{\mathrm{r}}(s) \\ &= \frac{\bar{c}}{s} \frac{\lambda^2}{4\pi d\alpha D} \exp\left(-\lambda d\sqrt{\frac{s}{D}}\right) \frac{k_{\mathrm{i}} a p_{\mathrm{m}} N}{(k_{\mathrm{d}} + s)(k_{\mathrm{i}} + s)}. \end{aligned} \quad (11)$$

To the best of the authors' knowledge, no closed-form solution exists for the inverse Laplace transform of (11). To overcome this limitation, we replace the exponential term in (11) by its Maclaurin series

$$\exp\left(-\lambda d\sqrt{\frac{s}{D}}\right) = 1 - \frac{\lambda d}{\sqrt{D}}\sqrt{s} + \frac{\lambda^2 d^2}{2D} s - \frac{\lambda^3 d^3}{6D^{3/2}} s^{3/2} + \dots. \quad (12)$$

By applying the inverse Laplace transform and considering the first order Maclaurin series, the received signal $y(t) \approx \bar{y}(t)$ can be approximated, where

$$\bar{y}(t) \approx \bar{c}\frac{\lambda^2 k_\mathrm{i} a p_\mathrm{m} N}{4\pi d\alpha D(k_\mathrm{d}^2 k_\mathrm{i} - k_\mathrm{d} k_\mathrm{i}^2)} \times \Theta(t) \times \left[\frac{2\lambda d\left(k_\mathrm{i}\sqrt{k_\mathrm{d}} F_\mathrm{D}\left(\sqrt{k_\mathrm{d} t}\right) - k_\mathrm{d}\sqrt{k_\mathrm{i}} F_\mathrm{D}\left(\sqrt{k_\mathrm{i} t}\right)\right)}{\sqrt{\pi D}} - k_\mathrm{d}\exp\left(-k_\mathrm{i} t\right) + k_\mathrm{i}\exp\left(-k_\mathrm{d} t\right) + k_\mathrm{d} - k_\mathrm{i}\right] \quad (13)$$

and $F_\mathrm{D}(\cdot)$ denotes the Dawson integral of the form

$$F_\mathrm{D}(x) = \exp\left(-x^2\right)\int_0^x \exp\left(z^2\right)\,\mathrm{d}z. \quad (14)$$

III. Drug Release Optimization

In TDD, there are several limitations in the system that must be taken into account. The most important ones can be summarized as follows:

- *Transmitter:* The release of EVs from the transmitter cell cannot be modulated arbitrarily. Since it is a biological process, the rate of release and concentration are limited. For example, a neuron, as assumed here, follows an all-or-nothing principle and only the frequency of generated action potentials can be controlled. Additionally, this frequency is upper bounded by the minimal refractory period. Furthermore, the transmitter cell contains only a finite amount of EVs and needs time for synthesizing new EVs. In this work, we assume that the transmitter will have a sufficient amount of EVs available after the minimal refractory period. In other words, EVs are not depleted at the time of action potentials. Given this assumption, the transmitter model from Sec. II-A can be applied. If EVs can get depleted, the transmitter model from Sec. II-A has to be extended by the synthesis rate of EVs and their storage within the cell. This may introduce a time dependency which has to be considered in the derivation of $y(t)$. To conserve the energy used for the generation of the induced current and to avoid a drop of the EV concentration at the receiver, the complete depletion of the EVs in the transmitter should be avoided. In this case the optimization problem introduced later in this section is still valid for an updated $y(t)$.
- *Channel:* In drug delivery, toxicity is an important effect. If the local concentration of a drug is too high, it can be harmful to (healthy) cells in the environment after uptake. In this work, we consider a special case where the drugs are encapsulated in EVs and propagate through the ECM. EVs can be target-specific and thus are assumed to be taken up only by the targeted cells. Thus, toxicity is not considered in this work.
- *Receiver:* The time that the drug is present at a specific concentration in the target cell determines the achieved therapeutic effect [19]. The therapeutic window indicates a range between an upper and a lower concentration threshold in which the drug concentration ideally should be during the entire duration of treatment. The lower threshold is defined by the least effective concentration. If the concentration falls below this threshold, the therapeutic effect can no longer be guaranteed. The upper threshold is defined by the efficacy. Due to a finite number of receptors and the time required for binding, only a finite number of EVs can be internalized by the target cell per time. Thus, an increase in concentration above the upper threshold will only result in a waste of drug-carrying EVs, whose quantity is also limited in the transmitter [6], [9].

In addition to holding a target concentration at the target cell for a certain period of time, reaching this concentration provides room for optimization. In this paper, we consider two different optimization approaches. In the first approach, the focus is on the fastest possible treatment. In this case, a target concentration should be reached as quickly as possible [6]. The second approach tries to optimize the resources used. Here, the amount of EVs released to reach the target concentration is to be minimized [7]. Depending on the disease and the applied delivery system, one of the two approaches will be of interest.

In the following, the optimization solutions are presented. A distinction is made between the steady state and rising state. The former deals with holding a target concentration while the latter deals with reaching the target concentration either fast or in a resource-efficient way.

A. Steady State Solution

Depending on the period T between the generated action potentials, a steady state with a constant uptake concentration level C_∞ will be reached after sufficient time. Using the final value theorem and (11) yields

$$\begin{aligned} C_\infty &= \lim_{t\to\infty} y(t) = \lim_{s\to 0} sY(s) \\ &= \left(c_\mathrm{min} + \frac{c_\mathrm{max} - c_\mathrm{min}}{\gamma T}\right)\frac{\lambda^2 a p_\mathrm{m} N}{4\pi d\alpha D k_\mathrm{d}}. \end{aligned} \quad (15)$$

Solving (15) for T, we obtain the required neuron excitation period

$$T_\infty = \frac{\frac{c_\mathrm{max}-c_\mathrm{min}}{\gamma}}{C_\mathrm{t}\frac{4\pi d\alpha D k_\mathrm{d}}{\lambda^2 a p_\mathrm{m} N} - c_\mathrm{min}}, \quad (16)$$

to hold a target uptake concentration C_t under steady state condition.

B. Rising State Solution

First, we consider the case where a target concentration is to be reached as fast as possible. Logically, in this case action potentials must be triggered at the neuron with the smallest possible period T, which is limited by the minimal refractory period. From the time when (13) reaches the desired EV uptake concentration C_t in the cancer cell, the stimulus is switched to the steady state solution and action potentials with period T_∞ are generated.

As shown later in Sec. IV and in Fig. 8, reaching the target concentration as fast as possible leads to a significant overshoot. Avoiding this overshoot leads to the resource efficient solution. To achieve this goal, the neuron's excitation is divided into three phases.

1: **procedure** OPTIMIZE($C_\mathrm{t}, \varepsilon, \overleftarrow{\tau}, \overrightarrow{\tau}, \overleftarrow{t_\mathrm{max}}, \overrightarrow{t_\mathrm{max}}$)
2: $\quad\tau \leftarrow (\overleftarrow{\tau} + \overrightarrow{\tau})/2$
3: $\quad t_\mathrm{max} \leftarrow$ maximize $f_\mathrm{r}(t,\tau)$ within $\overleftarrow{t_\mathrm{max}} < t < \overrightarrow{t_\mathrm{max}}$
4: $\quad C \leftarrow f_\mathrm{r}(t_\mathrm{max}, \tau)$
5: $\quad$ **if** $|C_\mathrm{t} - C| > \varepsilon$ **then** ▷ C_t not reached
6: $\quad\quad$ **if** $C > C_\mathrm{t}$ **then** ▷ Right side of optimum
7: $\quad\quad\quad$ OPTIMIZE($C_\mathrm{t}, \varepsilon, \overleftarrow{\tau}, \tau, \overleftarrow{t_\mathrm{max}}, t_\mathrm{max}$)
8: $\quad\quad$ **else** ▷ Left side of optimum
9: $\quad\quad\quad$ OPTIMIZE($C_\mathrm{t}, \varepsilon, \tau, \overrightarrow{\tau}, t_\mathrm{max}, \overrightarrow{t_\mathrm{max}}$)
10: $\quad\quad$ **end if**
11: $\quad$ **end if**
12: $\quad$ **return** τ, t_max
13: **end procedure**

Fig. 3. Recursive optimization algorithm based on bisection method to solve (18).

1) In the initial *rising phase*, the neuron is excited with T, which leads to an initial increase in EV concentration in the tumor cell.
2) At time τ, the *resting phase* begins, where the external signal, used to depolarize the neuron, is turned off. Consequently, no more EVs are released from the neuron than the baseline EV release rate c_min. The time τ is chosen such that the remaining increase in uptake concentration reaches its maximum with the target uptake concentration C_t at time point t_max.
3) At time point t_max, the maximum uptake concentration from the resting phase and thus also the target uptake concentration C_t is reached. Consequently, the external stimulus is switched to the *steady state phase*, where the neuron is excited with T_∞ and thus C_t is held.

We describe the initial concentration increase as a function of τ as

$$f_\mathrm{r}(t,\tau) = \bar{y}(t) - \bar{y}(t-\tau). \tag{17}$$

The optimal choice of τ such that at time t_max the target uptake concentration C_t is reached can be described by a bilevel optimization problem as

$$\begin{aligned} &\min_{\tau\in\mathbb{R}_{>0}} \left\{ \left(C_\mathrm{t} - f_\mathrm{r}(t_\mathrm{max},\tau)\right)^2 \right\}, \\ &\quad \text{subject to } t_\mathrm{max} \in \arg\max_{t\in\mathbb{R}_{>0}} \left\{ f_\mathrm{r}(t,\tau) \right\}. \end{aligned} \tag{18}$$

While the lower-level optimization describes the achieved uptake concentration maximum for given τ, the upper-level optimization ensures that the uptake concentration maximum coincides with the target uptake concentration C_t. As shown in the Appendix, the optimization problems are quasiconcave and quasiconvex, respectively. This property is essential to define (18) as optimum, because it ensures that only a single minimum and maximum respectively exists for each optimization level. Therefore, there is only a single t_max for each τ.

Unfortunately, direct computation of t_max is not possible and must be obtained by search algorithms. One approach is to nest two optimization methods, which describe the lower-level and upper-level optimization separately. The upper-level optimization can be solved recursively using the bisection method [20], as we demonstrate in Fig. 3. This takes advantage of the fact that $f_\mathrm{r}(t_\mathrm{max},\tau)$ is monotonically increasing with τ. By comparing $C = f_\mathrm{r}(t_\mathrm{max},\tau)$ with the target EV uptake concentration C_t, it can be determined whether the current τ is to the left or to the right of the optimum. Accordingly, the next search interval is chosen to be $[\tau, \overrightarrow{\tau}]$ or $[\overleftarrow{\tau}, \tau]$, which is expressed by the recursive call in either line 7 or line 9 in Fig. 3. The lower-level optimization (line 3 in Fig. 3) can be realized, for example, by the golden-section search algorithm [21], where the search interval can be bounded, since t_max is monotonically increasing with τ. Consequently, t_max lies between $\overleftarrow{t_\mathrm{max}}$ and $\overrightarrow{t_\mathrm{max}}$ of the left and right interval boundaries, respectively. The search for the optimum is completed when the deviation of C from C_t is smaller than a residual error ε.

TABLE I
DEFINITION OF MATHEMATICAL SYMBOLS AND CORRESPONDING VALUES FOR THE SCENARIO UNDER INVESTIGATION. NOTE THAT UNIT Mol REFERS TO THE NUMBER OF EVS OR PITS.

Parameter	Symbol	Value	Ref.
Neuron excitation period	T	$\geq 2\,\mathrm{ms}$	[16]
Maximum EV release rate	c_max		
Minimum EV release rate	c_min	$c_\mathrm{max}/10$	
Target EV uptake concentration	C_t	$c_\mathrm{max}/10^9$	
Exponential decay factor	γ	$59.91\,1/\mathrm{s}$	[3]
Free diffusion coefficient	D	$10\,\mu\mathrm{m}^2/\mathrm{s}$	[22]
Volume fraction brain ECM	α	0.2	[23]
Tortuosity brain ECM	λ	1.6	[23]
Transmission distance	d	$1\,\mu\mathrm{m}$	[2]
Rate of EVs binding to receptor	a	$6.64\times10^{-17}\,\mathrm{mL}/(\mathrm{Mol}\cdot\mathrm{s})$	[2]
Clathrin-coated pits concentration	N	$1.81\,\mathrm{Mol}/\mathrm{mL}$	[24]
Maximum receptors per pit	p_m	200	[24]
EV internalization rate	k_i	$0.0027\,1/\mathrm{s}$	[24]
EV degradation rate	k_d	$0.0002\,1/\mathrm{s}$	[24]

IV. NUMERICAL RESULTS

In the following, we first discuss the parameters selected for the obtained numerical results. Afterwards, we justify the approximations made for the derivation of the end-to-end model. Finally, we analyze the impact of the optimizations of the initial concentration rise presented in this work.

A. Parameter Selection

Within the numerical results, we attempt to reproduce as well as possible a realistic TDD scenario for brain tumors such as glioblastoma multiforme. Tab. I lists the parameters under investigation with their respective references. The transmitter is assumed to be a neuron whose excitation is limited by the minimal refractory period. As described in Section II-A, the release rate of EVs associated with action potentials is approximated using an exponential decay function. The exponential decay factor γ is estimated by the presented release rate results [3]. The diffusion coefficient is a typical value for EVs and the tortuosity and volume fraction are typical values for the ECM of the brain. Unfortunately, there is little work available in the literature on the parameterization of the endocytosis process and we are not aware of any work in this

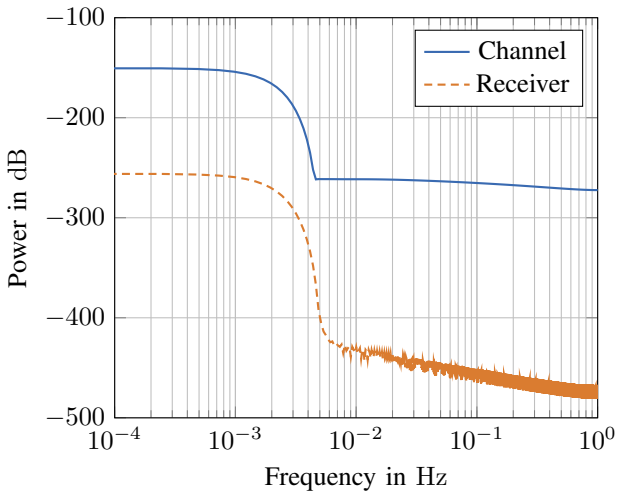

Fig. 4. Power spectra that demonstrate the low-pass filter characteristic of the diffusion channel and the receiver based on clathrin-dependent receptor-mediated endocytosis. Parameters are chosen according to Tab. I.

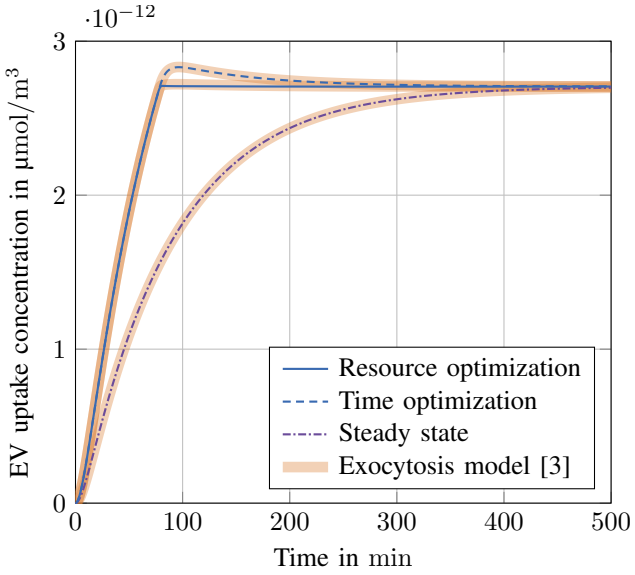

Fig. 5. EV concentration in the tumor cell for rising time optimization, resource optimization, and steady state solution. As a comparison, the numerical results of the exocytosis model presented in [3] are added. The parameters under investigation for exocytosis are taken from [3] with an induced control current of $i_{\mathrm{ind}} = 20\,\mu\mathrm{A/cm^2}$ for the rising phase and $i_{\mathrm{ind}} = 5\,\mu\mathrm{A/cm^2}$ for the steady state. Assuming a microdomain volume of $1\,\mathrm{mL}$, this leads to an average release rate of $\bar{c} = 3.86 \times 10^{-3}\,\mu\mathrm{mol/s}$ and $\bar{c} = 2.23 \times 10^{-3}\,\mu\mathrm{mol/s}$, respectively, which is used in the end-to-end model derived in this paper. Channel and endocytosis parameters are listed in Tab. I.

regard with respect to brain tumor cells. Therefore, we take the receiver parameters from references dealing with hepatocytes instead [2], [24]. While the parameters for glioblastoma cells may be different, the mechanics of endocytosis are still the same. Thus, it is to be expected that the system model can be adapted to new specific values of the parameters with little effort. Furthermore, experimental work is often performed in cultured cells. Thus, the exact EV concentration in organisms remains unclear [25]. Therefore, in this work, release rates and uptake concentrations are given relative to $c_{\max}$.

B. Channel Assumptions

We made two approximations to derive the end-to-end model presented in Sec. II, which are analyzed and justified here by means of numerical results.

The first approximation concerns the exact mathematical description of the exocytosis at the transmitter side. Since the internalization of EVs in endocytosis is the rate-limiting process and comparatively much slower than the release of EVs by exocytosis [18], the exact dynamics of the EV release has minimal influence and can be replaced by its averaged dynamics in (10). This observation is also reflected when examining the power spectra of the channel and the receiver in Fig. 4. In fact, the channel and the receiver show a low-pass filter behavior. The receiver-side endocytosis and internalization react as a second-order low-pass filter, see also (7). To further justify the inclusion of only the averaged dynamics of exocytosis in the system model, Fig. 5 compares the obtained results of the optimization strategies presented in this work with a numerical calculation considering the complete exocytosis model and parameters from [3]. An induced control current of $i_{\mathrm{ind}} = 20\,\mu\mathrm{A/cm^2}$ is assumed for the rising phase and $i_{\mathrm{ind}} = 5\,\mu\mathrm{A/cm^2}$ for a steady state. Assuming a microdomain volume of $1\,\mathrm{mL}$, this corresponds to an average release rate of $\bar{c} = 3.86 \times 10^{-3}\,\mu\mathrm{mol/s}$ and $\bar{c} = 2.23 \times 10^{-3}\,\mu\mathrm{mol/s}$, respectively. Fig. 5 demonstrates that the simplification through approximation is in good agreement with the results obtained using the entire exocytosis model. In fact, the maximum normalized squared error is 2.58×10^{-5} and occurs in resource optimization at the transition to the steady state phase. The more detailed analysis of the different optimization strategies is elaborated in Sec. IV-C and is therefore omitted here.

The second approximation involves substituting the exponential term using the first order Maclaurin series in (12). Fig. 6 shows the approximation accuracy in comparison to a numerically obtained inverse Laplace transform of (9), taking into account the parameters listed in Tab. I. At least for the scenario under investigation, it can be observed that the Maclaurin series of the first order already offer a sufficiently accurate approximation and is therefore applied throughout the rest of the paper. As a comparison, the normalized squared error taking into account the Maclaurin series of the second and third order is also shown. In these two cases, the inverse Laplace transform is determined numerically and not by an analytical solution. It can be observed that the approximation becomes more accurate with increasing order. Further justification for the approximation accuracy is provided in Fig. 5. While the optimization results are based on the end-to-end model (13), the results considering the exact exocytosis model are based on the convolution in time domain according to (8), thereby avoiding the approximation by the Maclaurin series. The good agreement of the results further demonstrates the sufficient accuracy of the approximation performed.

So far we have shown that the two approximations are reasonable for the parameters under investigation. In the

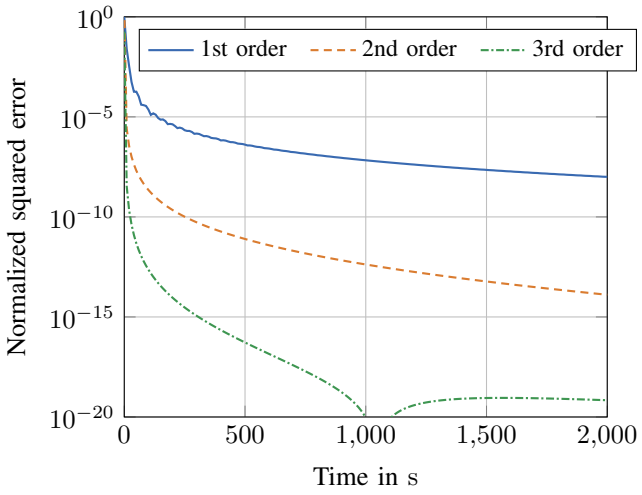

Fig. 6. Normalized squared error between numerically determined inverse Laplace transform of $\boldsymbol{Y}(\boldsymbol{s})$ and first order Maclaurin series approximated solution $\bar{\boldsymbol{y}}(\boldsymbol{t})$. The inverse Laplace transform of the second and third order are also determined numerically. Parameters are chosen according to Tab. I and $\boldsymbol{T} = 1\,\mathrm{s}$.

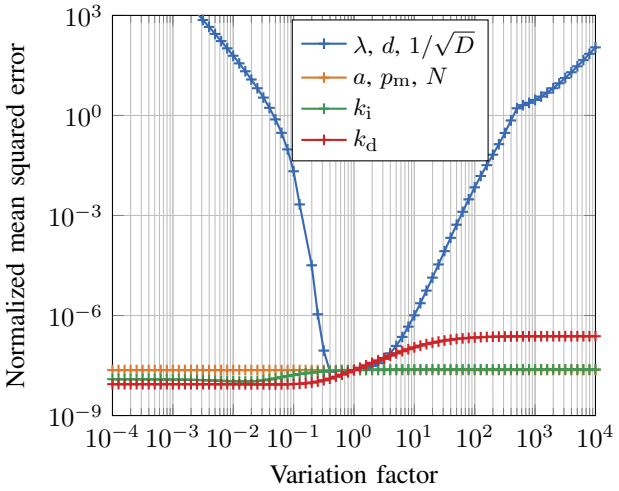

Fig. 7. Impact of parameter variations on the normalized mean squared error between numerically determined inverse Laplace transform of $\boldsymbol{Y}(\boldsymbol{s})$ including exocytosis model presented in [3] and first order Maclaurin series approximated solution $\bar{\boldsymbol{y}}(\boldsymbol{t})$ assuming averaged EV release rate. Parameter variation is described by a variation factor multiplied by the channel and endocytosis parameters listed in Tab. I. For the exocytosis model, the steady-state scenario in Fig. 5 is used.

following, we want to analyze the validity of the two approximations when the parameters are varied. For this purpose we consider the steady state scenario from Fig. 5 and vary channel and endocytosis parameters by multiplying a variation factor. To evaluate the validity of the approximation, we calculate the normalized mean squared error (NMSE) between $\bar{y}(t)$ and the numerical inverse Laplace transform of $Y(s)$ considering the exocytosis model from [3]. In Fig. 7 it is evident that the NMSE is mainly influenced by λ, d and D. As shown in (12), the terms of higher orders gain influence when λ and d are increased, or D is decreased. Consequently, the error increases by considering only the first order term in $\bar{y}(t)$. The increasing NMSE with decreasing variation factor is due to

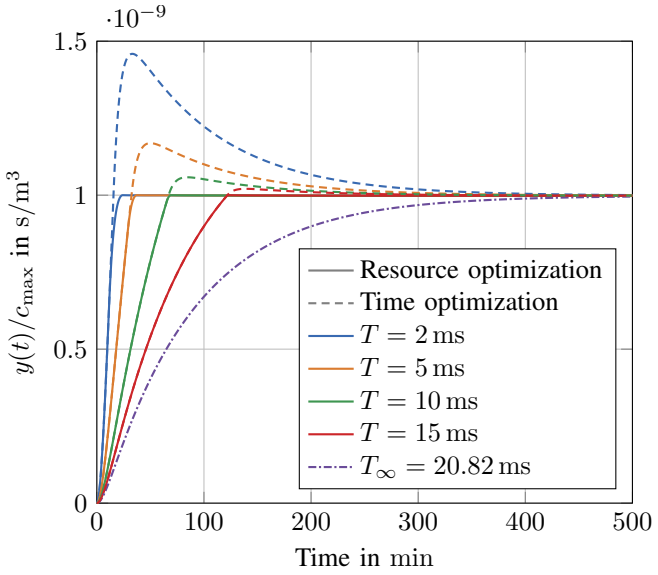

Fig. 8. EV concentration in the tumor cell for rising time and resource optimization at different excitation periods $\boldsymbol{T}$. The parameters under investigation are summarized in Tab. I.

numerical limitations instead of the performed approximation. For decreasing d, λ, or increasing D, the shape of h_c becomes increasingly impulsive. In order to reflect this shape correctly in the numerical Laplace transform, the temporal resolution must theoretically be increased which would lower the NMSE. Practically, however, the temporal resolution cannot be increased arbitrarily. A variation of a, p_m, and N does not affect the NMSE, since they act only as factors in (11) and their variation is compensated by the normalization in the NMSE. The same applies also to λ, d, and D outside the exponential term in (11). If k_i and k_d are varied, the low-pass characteristic of the endocytosis process is affected. An increase of the chemical reaction rates leads to an increase of the cutoff frequency and relatively less attenuation of higher frequency components. Consequently, the exact time course of the transmitted signal becomes more important and the NMSE increases. The NMSE increases, however, only to a limited extent, since the channel still features a low-pass characteristic as well. In conclusion, the approximations made in this work are reasonable over a wide range of parameters.

C. Optimization Analysis

Fig. 8 shows the EV uptake concentration profiles in the target cell for the two different optimizations and different excitation intervals. As expected, the target concentration is reached fastest when the smallest possible excitation interval $T = 2\,\mathrm{ms}$ is applied until $y(t) = C_\mathrm{t}$ (see also Fig. 9). The change to $T_\infty = 20.82\,\mathrm{ms}$ calculated according to (16) already occurs after $16\,\mathrm{min}$. In comparison, the target concentration is almost reached after $500\,\mathrm{min}$ for continuous excitation with T_∞. Since endocytosis is a slow process, the fast increase results in an overshoot. This overshoot decreases with increasing T and disappears with continuous excitation with T_∞.

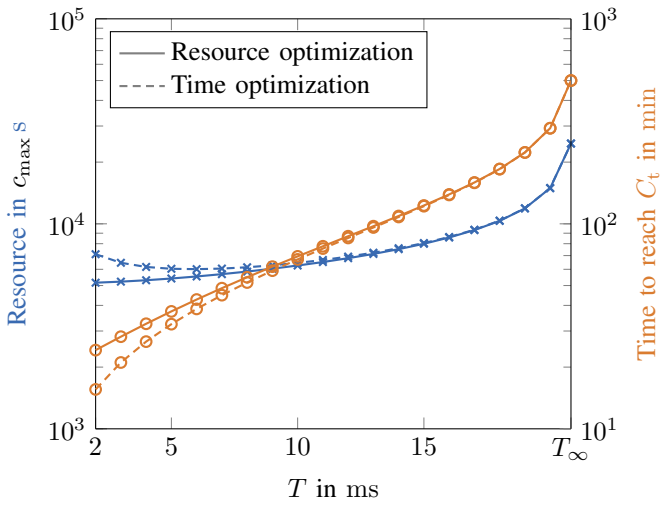

Fig. 9. Required resources and time to reach the target concentration C_t for the resource optimization and the time optimization as a function of the excitation period T. The parameters under investigation are given in Tab. I.

The resource-efficient approach according to (18) prevents overshoot entirely by its resting phase and simultaneously concerves EVs. Fig. 9 shows the required resources by the different approaches to reach the target uptake concentration C_t as a function of the excitation period T. For this purpose, the resources are represented by the EV release rate multiplied by the time required to reach it. In addition, the time needed to reach C_t is depicted over T. Here it can be seen that also for the optimization according to (18), the excitation interval T should be chosen as small as possible. The minimum resource consumption is $5162\,c_{\max}\,\mathrm{s}$ for initial excitation with $T = 2\,\mathrm{ms}$, whereas the maximum resource consumption is $24642\,c_{\max}\,\mathrm{s}$ for continuous excitation with T_∞. The target concentration is reached after $24\,\mathrm{min}$.

V. Conclusion

This work considers an EV-based TDD scenario for the treatment of glioblastoma multiforme as a case study. In this context, the transmitter is modeled as an excitable neuron which releases therapeutic EVs, and the receiver is modeled as a sick glioblastoma cell which takes up EVs from the ECM of the brain via the clathrin-dependent endocytosis. To describe the input-output behavior of the system, the transfer function is formulated in the Laplace domain. Based on the transfer function, an analytical solution in the time domain is derived and verified by numerical results. The analytical solution is used to optimize the stimulation of the neuron, including the release of the drug carrying EVs, with respect to the concentration of internalized EVs in the glioblastoma cell. The focus is on either the fastest possible treatment or a drug-saving treatment. The latter is formulated as a bilevel optimization problem and its quasiconvex/quasiconcave property is proved. A solving algorithm is proposed by a combination of bisection method and golden-section search. The numerical results demonstrate the great potential of the optimization. For the scenario under investigation, the time to reach the therapeutic target concentration can be shortened by a factor of ≥ 32 compared to the steady state solution. Alternatively, the required EVs to reach the target concentration can be reduced by a factor of ≥ 4.7. It should be mentioned that the derived end-to-end model is applied here to optimize TDD, but is not limited to it. It provides the community a more realistic model described by an analytical solution in the time domain for intercellular communication scenarios by taking into account effects such as tortuosity and volume fraction, and physiological mechanisms such as exocytosis and endocytosis.

Future works include an extension to a network of neurons and glioblastoma cells and an enhanced modeling of the transmitter. Besides the consideration of astrocytes, the exact dynamics of exocytosis [3] can be included in the end-to-end model. Furthermore, modeling of EV synthesis in neurons and its resulting limitation would be of interest.

Appendix

All parameters in (13) describe nonnegative physical phenomena. Furthermore, $\bar{y}(0) = 0$ and $\bar{y}(\infty) = C_\infty$ applies. In between, $\bar{y}$ is monotonically increasing because

$$\frac{1}{\sqrt{t}} > \frac{1}{\sqrt{t+\epsilon}} \quad \text{and} \quad \exp(-t) > \exp(-(t+\epsilon)), \tag{19}$$

and the Dawson integral can be approximated by

$$F_\mathrm{D}(z) \approx \begin{cases} z & \text{if } z \text{ is small} \\ 1/(2z) & \text{if } z \text{ is large} \end{cases}. \tag{20}$$

Consequently, it is added/subtracted less and less to/from $k_\mathrm{d} - k_\mathrm{i}$ with increasing t in (13), which results in a monotonic increase. Subtracting a time-shifted version of the monotonically increasing and converging function $\bar{y}(t)$ from itself in (17), leads to a unimodal function with a single global maximum whose value increases with τ. Consequently, also $f_\mathrm{r}(t_{\max}, \tau)$ is a monotonically increasing function and $(C_\mathrm{t} - f_\mathrm{r}(t_{\max}, \tau))^2$ results in a unimodal expression with a single global minimum. The unimodality properties are already sufficient to guarantee a unique solution to the optimization problem. Beyond that are all unimodal functions with a global minimum quasiconvex [26]. Consequently are $-f_\mathrm{r}(t, \tau)$ and $(C_\mathrm{t} - f_\mathrm{r}(t_{\max}, \tau))^2$ quasiconvex, which indicates that $f_\mathrm{r}(t, \tau)$ is quasiconcave.

References

[1] U. A. K. Chude-Okonkwo, R. Malekian, B. T. Maharaj, and A. V. Vasilakos, "Molecular communication and nanonetwork for targeted drug delivery: A survey," *IEEE Commun. Surveys Tutorials*, vol. 19, no. 4, pp. 3046–3096, fourthquarter 2017.

[2] M. Veletić, M. T. Barros, I. Balasingham, and S. Balasubramaniam, "A molecular communication model of exosome-mediated brain drug delivery," in *Proc. ACM Int. Conf. on Nanoscale Computing and Communication (NANOCOM)*, Dublin, Ireland, Sep. 2019, p. 1–7.

[3] M. Veletić, M. T. Barros, H. Arjmandi, S. Balasubramaniam, and I. Balasingham, "Modeling of modulated exosome release from differentiated induced neural stem cells for targeted drug delivery," *IEEE Trans. Nanobiosci.*, vol. 19, pp. 357–367, Jul. 2020.

[4] Y. Chen, Y. Zhou, R. Murch, and P. Kosmas, "Modeling contrast-imaging-assisted optimal targeted drug delivery: A touchable communication channel estimation and waveform design perspective," *IEEE Trans. Nanobiosci.*, vol. 16, no. 3, pp. 203–215, Apr. 2017.

[5] H. K. Rudsari, N. Mokari, M. R. Javan, E. A. Jorswieck, and M. Orooji, "Drug release management for dynamic TDMA-based molecular communication," *IEEE Trans. Mol. Biol. Multi-Scale Commun.*, vol. 5, no. 3, pp. 233–246, Dec. 2019.
[6] T. Nakano, Y. Okaie, and A. V. Vasilakos, "Transmission rate control for molecular communication among biological nanomachines," *IEEE J. Sel. Areas Commun.*, vol. 31, no. 12, pp. 835–846, Dec. 2013.
[7] S. Salehi, N. S. Moayedian, S. S. Assaf, R. G. Cid-Fuentes, J. Solé-Pareta, and E. Alarcón, "Releasing rate optimization in a single and multiple transmitter local drug delivery system with limited resources," *Nano Communication Networks*, vol. 11, pp. 114–122, Mar. 2017.
[8] Q. Zhao and L. Lin, "Adaptive release rate in drug delivery based on mobile molecular communication," in *Proc. IEEE Wireless Communications and Networking Conf. (WCNC)*, Nanjing, China, Mar. 2021, pp. 1–6.
[9] Q. Zhao, M. Li, and L. Lin, "Release rate optimization in molecular communication for local nanomachine-based targeted drug delivery," *IEEE Trans. Nanobiosci.*, vol. 20, no. 4, pp. 396–405, Oct. 2021.
[10] J. Fauré, G. Lachenal, M. Court, J. Hirrlinger, C. Chatellard-Causse, B. Blot, J. Grange, G. Schoehn, Y. Goldberg, V. Boyer, F. Kirchhoff, G. Raposo, J. Garin, and R. Sadoul, "Exosomes are released by cultured cortical neurones," *Molecular and Cellular Neuroscience*, vol. 31, no. 4, pp. 642–648, Apr. 2006.
[11] E. J. Bunggulawa, W. Wang, T. Yin, N. Wang, C. Durkan, Y. Wang, and G. Wang, "Recent advancements in the use of exosomes as drug delivery systems," *Journal of Nanobiotechnology*, vol. 16, no. 1, pp. 1–13, Oct. 2018.
[12] L. R. Galieva, V. James, Y. O. Mukhamedshina, and A. A. Rizvanov, "Therapeutic potential of extracellular vesicles for the treatment of nerve disorders," *Frontiers in Neuroscience*, vol. 13, pp. 1–9, Mar. 2019.
[13] J. R. Bagó, A. Alfonso-Pecchio, O. Okolie, R. Dumitru, A. Rinkenbaugh, A. S. Baldwin, C. R. Miller, S. T. Magness, and S. D. Hingtgen, "Therapeutically engineered induced neural stem cells are tumour-homing and inhibit progression of glioblastoma." *Nature communications*, vol. 7, p. 10593, Feb. 2016.
[14] K. Hemmer, M. Zhang, T. van Wüllen, M. Sakalem, N. Tapia, A. Baumuratov, C. Kaltschmidt, B. Kaltschmidt, H. R. Schöler, W. Zhang, and J. C. Schwamborn, "Induced neural stem cells achieve long-term survival and functional integration in the adult mouse brain." *Stem cell reports*, vol. 3, pp. 423–431, Sep. 2014.
[15] M. Ruggieri, G. Riboldi, S. Brajkovic, M. Bucchia, N. Bresolin, G. P. Comi, and S. Corti, "Induced neural stem cells: Methods of reprogramming and potential therapeutic applications," *Progress in Neurobiology*, vol. 114, pp. 15–24, Mar. 2014.
[16] S. Sardi, R. Vardi, Y. Tugendhaft, A. Sheinin, A. Goldental, and I. Kanter, "Long anisotropic absolute refractory periods with rapid rise times to reliable responsiveness," *Phys. Rev. E*, vol. 105, p. 014401, Jan. 2022.
[17] G. Lachenal, K. Pernet-Gallay, M. Chivet, F. J. Hemming, A. Belly, G. Bodon, B. Blot, G. Haase, Y. Goldberg, and R. Sadoul, "Release of exosomes from differentiated neurons and its regulation by synaptic glutamatergic activity," *Molecular and Cellular Neuroscience*, vol. 46, no. 2, pp. 409–418, Feb. 2011.
[18] H. J. Harwood Jr and L. D. Pellarin, "Kinetics of low-density lipoprotein receptor activity in Hep-G2 cells: derivation and validation of a Briggs–Haldane-based kinetic model for evaluating receptor-mediated endocytotic processes in which receptors recycle," *Biochemical Journal*, vol. 323, no. 3, pp. 649–659, May 1997.
[19] T. M. Allen and P. R. Cullis, "Drug delivery systems: Entering the mainstream," *Science*, vol. 303, no. 5665, pp. 1818–1822, Mar. 2004.
[20] S. D. Conte and C. De Boor, *Elementary numerical analysis: an algorithmic approach*. Society for Industrial and Applied Mathematics, 2017.
[21] R. P. Brent, *Algorithms for minimization without derivatives*. Courier Corporation, 2013.
[22] N. Kastelowitz and H. Yin, "Exosomes and microvesicles: Identification and targeting by particle size and lipid chemical probes," *ChemBioChem*, vol. 15, no. 7, pp. 923–928, May 2014.
[23] E. Syková and C. Nicholson, "Diffusion in brain extracellular space," *Physiological Reviews*, vol. 88, no. 4, pp. 1277–1340, Oct. 2008.
[24] J. Wattis, B. O'Malley, H. Blackburn, L. Pickersgill, J. Panovska, H. Byrne, and K. Jackson, "Mathematical model for low density lipoprotein (ldl) endocytosis by hepatocytes," *Bulletin of Mathematical Biology*, vol. 70, no. 8, pp. 2303–2333, Aug. 2008.
[25] V. Budnik, C. Ruiz-Cañada, and F. Wendler, "Extracellular vesicles round off communication in the nervous system," *Nature Reviews Neuroscience*, vol. 17, no. 3, pp. 160–172, Mar. 2016.
[26] S. Boyd and L. Vandenberghe, *Convex Optimization*. Cambridge University Press, 2004.